Proceedings of the ASME 2010 3rd Joint US-European Fluids Engineering Summer Meeting and 8th International Conference on Nanochannels, Microchannels, and Minichannels
FEDSM-ICNMM2010
August 1-5, 2010, Montreal, Canada

FEDSM-ICNMM2010-30145

NUMERICAL INVESTIGATION AND GEOMETRIC PARAMETERIZATION OF LAMINATION INLET OF PASSIVE MICROMIXER

Yanfeng Fan
Department of Mechanical and Industrial Engineering,
Concordia University, Montreal, Quebec, Canada
H3G1M8
f_yanfen@encs.concordia.ca

Ibrahim Hassan[1]
Department of Mechanical and Industrial Engineering,
Concordia University, Montreal, Quebec, Canada
H3G1M8
ibrahimh@alcor.concordia.ca

ABSTRACT
A lamination inlet is proposed and optimized in this paper. The perpendicular incoming fluids are applied instead of parallel type. The total mixing length is fixed at 3.2 mm and the depth of channel is fixed at 0.1 mm. The tested Reynolds number is calculated at the entrance of downstream straight channel. The tested Reynolds numbers range from 5 to 200. The perpendicular incoming type enhances the mass-convection and enlarges the interface area. Two parameters, the radius of holes (R) and the distance between two holes (D_1), are selected to achieve the optimization. Numerical simulation is used to estimate the mixing performance and flow characteristics. The results show that the vortices are generated in the microchannel. The interface becomes irregular. In order to evaluate the mixing improvement, the parallel lamination is also simulated. The comparison shows that the perpendicular inlet type has better mixing efficiency than the parallel lamination type. This inlet type could be connected with certain mixing element to achieve the applications in biochemistry.

INTRODUCTION
Microfluidic mixing applications have expanded into many fields, including medical drug delivery, biological, chemical and thermal applications. An assortment of micro devices have been designed and developed to complete microsystems, such as micro heat sinks and micro pumps. Micromixers remain, however, an indispensable component for the realization of microsystems. They have been widely utilized in micro total analysis systems (μTAS) and lab-on-a-chip systems for biological analysis, chemical synthesis and clinical diagnostics [1, 2]. Fluid flow and mass transfer mechanisms in microfluidic mixers are of great importance, and must be developed in order to satisfy the requirements of micro devices. Due to large pressure drop inside the microchannels, mixing becomes a very difficult task to accomplish, as the flow is characterized as laminar flow. Compared with turbulent flow, the mixing efficiency in micromixers is very low, as mixing relies mainly on molecular diffusion. In order to efficiently and effectively operate in these practical applications, ideal micromixers, which have rapid mixing, high mixing efficiency and low pressure drop, are required to satisfy future developments at the micro-scale.

Depending on the mixing mechanism, micromixers are classified into two categories: active micromixers and passive micromixers. Because of external power requirements and high cost, active micromixers are not good options for microsystem applications. Passive micromixers do not have moving parts, and rely on the geometry of microchannels, instead of an external power source, to enhance mixing. Since passive micromixers have a simple manufacturing process, are less costly, and may be easily implemented in microsystems, they are preferable for future applications. Many kinds of passive micromixers have emerged. These micromixers have utilized different methods to improve mixing efficiency, including 3D structure [3] and 2D structure [4, 5].

The interdigital lamination structure is used to design the passive micromixers to increase the interface and decrease the diffusion path. The principle is to divide the main flow into *n* substreams and these substreams recombine together to create the interdigital flow pattern causing diffusion to occur faster. The interdigital micromixers have been designed and investigated experimentally [6-11] and theoretically [12-14]. Koch et al. [6] proposed two different micromixers with lateral and vertical mixing based on the lamination principle. The first mixer separated the main flow into partial flows, which were laterally alternated in order to increase the boundary surface between the liquids. The second mixer superposed two fluids by injection of one liquid into the other. Similar concept of lateral mixing was applied in the micromixer presented by Bessoth et al. [7]. The two working fluids were divided into many substreams before mixing. Then the substreams combined together to complete the interdigital flow pattern in

[1] Author to whom correspondence should be addressed, E-mail: ibrahimh@alcor.concordia.ca

order to increase the interface and reduce the diffusion length compared with T-shape micromixer. The mixing regime was selected as straight channel. After 15ms, the mixing efficiency could reach 95%. Also, Bessoth et al. [7] firstly mentioned the effect of laminar width distribution on the mixing. They proposed that the relatively long time between a high percentage of mixing being achieved and completion was due to the fact that the fluid laminae at the edge of the channel are thicker than the ones in the center. Diffusion occurs in both directions, apart from the outermost laminae which can only mix with one neighbouring layer. However, there was no progress on the modification based on the concept. In order to improve the mixing performance of interdigital micromixers, Hessel et al. [9] and Hardt and Schönfeld [8] individually experimentally and numerically investigated four interdigital structure micromixers with different focusing regimes: rectangular, triangle, slit-shaped and superfocus. The uniform lamellae were applied and the lamellar number of each species was fixed as fifteen. The micromixer with superfocus regime achieved the mixing better than others and was considered as optimal design. The optimization of superfocus mixer was performed with an analytical model in creeping laminar flow regime by Drese [12]. Both focusing section and mixing channel were analyzed to find out the influence of design dimensions of mixer on the mixing quality. Each lamina had a constant width of 0.1mm for both species and opening angle was 50°. The width and length of mixing channel were discussed according to the height of mixing channel and pressure drop. All analysis was based on the fixed mixing quality as 99%. Increasing the pressure drop induced the reduced mixing quality in the focusing regime. When the height of channel was beyond a critical value at each pressure drop, the effect of channel height disappeared. The critical value decreased along the increased pressure drop. Cerbelli and Giona [14] analyzed the dynamics of mixing that took place in the mixing channel downstream the interdigital apparatus with rectangular focusing regime. The mixing length was estimated through mathematics model discussion. Three different flow profiles at inlet, which were plug, shear and Poiseuille flow, were applied to find out the effect of flow profile on mixing length. The mixing length was affected significantly by the flow profile at high degree of lamination of feed stream and no obviously by the lamellar thickness. However, all work mentioned above only focused on the focusing structure and mixing length, and showed bad mixing quality near the inner wall.

All mentioned above only focus on the parallel type. In this paper, the perpendicular inlet is investigated and optimized using CFD software. The grid independence is performed to minimize the effect of numerical diffusion. The tested range of Reynolds numbers are from 5 to 200.

MICROMIXER DESIGN

Figure 1 shows the schematic of the proposed passive micromixer. One species is pushed into the channel from the inlet, and the other species is pushed through several small holes located at the top of surface. Due to the smaller inlet areas, the blue species has larger velocity than the red species. The blue species punches into the red species, which induces a larger contact area. The perpendicular velocities of two species could enhance the mass-convection. The total mixing length is fixed at 3.2 mm. The upstream width of channel is 0.4 mm and downstream width is 0.1 mm. The depth of microchannel is maintained at 0.1 mm. The tested Reynolds number is calculated at the cross-section C2, as shown in Fig. 1.

NUMERICAL SIMULATION

Due to the symmetric structure, a half model is built and meshed in order to reduce the calculation time. The grid system and the symmetrical plane are shown in Fig. 2 Fluent® 6.3 is applied to simulate this model and evaluate the mixing performance. Only mixing occurs in the micromixer without chemical reactions. Hence, the reaction heat transfer may be cancelled. In order to simplify simulations, some assumptions are proposed before doing the simulation. The two fluids have same density and viscosity, and the variations of the concentration do not modify the density and viscosity of fluid. The flow can be viewed as steady-state and incompressible. No-slip boundary conditions exist at inner walls. Body force is neglected due to micro-scale dimension. According to the assumptions, the governing equations that contain continuity equation, Navier-Stokes equation and species advection-diffusion equation are represented as:

$$\nabla \cdot \boldsymbol{V} = 0\,, \tag{1}$$

$$\rho \boldsymbol{V} \cdot \nabla \boldsymbol{V} = -\nabla \boldsymbol{P} + \mu \nabla^2 \boldsymbol{V}\,, \tag{2}$$

$$\boldsymbol{V} \cdot \nabla C = D \nabla^2 C\,. \tag{3}$$

where $\boldsymbol{V}$ is the velocity vector and $\boldsymbol{P}$ is the pressure. The Navier-Stokes equation and continuity equation can be solved to get velocity in case of an incompressible fluid. The velocity is substituted into advection-diffusion equation to solve the concentration distribution.

Species transport model is selected to solve this case. Two species are defined in material options. One species is determined as pure water, whose density and viscosity are set at 10^3 kg/m^3 and 10^{-3} kg/m·s. A new species, named "dye", is defined to mix with pure water. It has same values of density and viscosity with water. The diffusion coefficient of dye in water is fixed at 1×10^{-10} m^2/s. Because there is no heat transfer, the energy equation is cancelled. The operating pressure is fixed at 10^5 Pa. The "velocity-inlet" type is assigned at two inlets. The velocity direction is normal to the boundary. Both inlet flows have same mass flow rate which are calculated through different tested Reynolds numbers. The concentrations of dye at two inlets are set at 0 and 1, respectively. The ideal mixing means the concentration of dye reaches 0.5. The outlet boundary is set at "pressure-outlet". The reference pressure is fixed at zero. The "SIMPLEC" module is applied for pressure-velocity coupling analysis of two mixing flows in microchannels. The discretization is "third-order QUICK" for velocity and species, and "second-order upwind" for pressure. The initial values of velocity and gauge pressure are set at zero. The maximum number of iteration is set at 3000 and the absolute convergence criterion is 10^{-6} for continuity, velocity, and species in order to get stable results. The grid independence is done to minimize the effect of numerical diffusion. The model is meshed at the grid numbers ranging from 0.2 M to 0.75 M. Figure 3 shows the concentration distribution at the intersection between the outlet and the center plane. The grid number of 0.59 M may be viewed as optimal and used for the further investigation. The parameter of mixing efficiency M is used to investigate the mixing process in the micromixer [5]. The expression is given as,

$$M = 1 - \sqrt{\frac{1}{N}\sum_{i=1}^{N}\left(\frac{c_i - \bar{c}}{\bar{c}}\right)^2}\ . \qquad (4)$$

where N is the total number of sampling mesh cells in a channel cross-section, c_i is the concentration at ith position, and $\bar{c}$ is the average concentration. The mixing efficiency is calculated at outlet. The value of mixing efficiency ranges from 0 (no mixing) to 1 (totally mixing).

RESULTS AND DISCUSSIONS

In order to find the mixing-enhancing geometry, two parameters are selected and three levels for each parameter are determined, as listed in Tab. 1. Nine cases are simulated at Re = 100. The mixing efficiency is calculated at the outlet using Eq. 4. Table 2 lists the results of mixing efficiency and pressure drop of nine cases. Case 2 shows the best mixing efficiency. The pressure drops among the nine cases are lower than 9 kPa. The concentration distributions are shown in Fig. 4. in order to investigate the influence of each parameter on the mixing. In Case 1, 2 and 3, the diameters of holes at the top of channel are same, and distance between two holes are set at 0.08 mm, 0.1 mm and 0.12 mm, respectively. Due to the high velocity, the blue species reach the bottom of the channel, and are reflected. The vortices are generated to stir the fluids in order to enhance the mass-convection. In Case 1, the space between two holes is small. The effective vortices could not be created. Also, the distance between the hole and the side wall is too large that the vortex may not influence the fluids near the side wall. In Case 3, the similar problem is observed. The space between two holes is large. A portion of red species is not affected by the vortex. However, the effective vortices are created both sides of holes in Case 2. The distance between holes is determined at 0.1 mm. Case 5 and 8 are selected to investigate the influence of diameter of holes on the mixing. At same Reynolds number, increasing the diameter may decrease the velocity of blue species, which induces the decreasing kinetic energy. In Case 5, the smaller velocity could not generate the folding of two species. In Case8, the blue species even cannot arrive at the bottom of channel. Therefore, the smaller diameter leads to the stronger vortices. The final design is determined as Case 2.

Figure 5 shows the concentration distributions at C1 in the entire range of tested Reynolds numbers. At low Reynolds number, the blue species could not touch the bottom of channel. However, the blue species is covered by the red species. As Re increases, the interface is increased. As soon as the blue species touch the bottom, the reflected fluids generate the vortices so that the mass-convection is enhanced. The larger Reynolds number results in the stronger vortices, as shown in Fig. 5.

In order to show the advantage of perpendicular inlet, parallel inlet is first simulated and investigated. Three substreams are applied and the channel area of each substream maintains same as one in the perpendicular inlet. Figure 6 shows the concentration distributions at C1 in the range of Reynolds numbers from 5 to 200. The interface keeps straight and the concentration gradient is along the horizontal direction. The velocity along the horizontal direction is so small that can not induce strong mass-convection. There are no vortices generated. The major mixing mechanism is mass-diffusion. Furthermore, the concentration profiles among the tested Reynolds numbers are almost same.

The mixing efficiency and pressure drop is shown in Fig. 7. As Re increases, the mixing efficiency increases even if the diffusion time is reduced. The mass-convection is dominant at the entire tested Reynolds numbers. The mixing efficiency of parallel inlet is lower than 20%. However, the mixing efficiency of perpendicular inlet is larger than 20% except Re = 5. The pressure drops of both inlet types are almost same. Therefore, the proposed inlet has better mixing performance than the previous lamination inlet.

CONCLUSIONS

In this paper, a novel lamination inlet was designed and investigated by numerical simulation. The one species was supplied from the top of the channel. The two species encountered and the velocities are perpendicular in order to enhance the mass-convection in the focusing part. The species from the top of channel was covered by the other one from the main channel at low Re. However, the reflected flow was generated and the vortices were created at high Re. Furthermore, the vortices became stronger as Re increases. The mixing efficiency increased along Re increased. The mass-convection was dominant in the entire tested Reynolds numbers. Compared with the parallel lamination inlet, the perpendicular inlet had better mixing performance and simplified the fabrication. The proposed inlet has potential to be used as inlet in biochemistry. By connecting the mixing element, the mixing efficiency could be improved.

REFERENCES

[1] Erickson, D. (2005). Towards numerical prototyping of labs-on-chip: modeling for integrated microfluidic devices. Microfluidics and Nanofluidics, 1, 301–318.

[2] Stone, H. A., Stroock, A. D., & Ajdari, A. (2004). Engineering flows in small devices: microfluidics toward a lab-on-a-chip. Annual review of fluid mechanics, 36, 381-411.

[3] Park, J. M., Kim, D. S., & Kang, T. G. (2007). Improved serpentine laminating micromixer with enhanced local advection. Microfluidics and Nanofluidics, 4, 513-523.

[4] Chung, C. K., & Shih, T. R. (2008). Effect of geometry on fluid mixing of the rhombic micromixers. Microfluidics and Nanofluidics, 4, 419-425.

[5] Shih, T. R., & Chung, C. K. (2007). A high-efficiency planar micromixer with convection and diffusion mixing over a wide Reynolds number range. Microfluidics and Nanofluidics, 5, 175-183.

[6] Koch, M., Chatelain, D., Evans, A. G. R., & Brunnschweiler, A. (1998). Two simple micromixers based on silicon, Journal of Micromechanics and Microengineering, 8, 123-6.

[7] Bessoth, F. G., deMello A. J., & Manz, A. (1999). Microstructure for efficient continuous flow mixing, Anal. Commun, 36, 213 – 215.

[8] Hardt, S. and Schönfeld, F. (2003). Laminar mixing in different interdigital micromixers: II. Numerical simulations, AIChE Journal, 49, 578-584.

[9] Hessel, V., Hardt, S., Löwe, H., & Schönfeld, F. (2003) Laminar mixing in different interdigital micromixers: I. Experimental characterization, AIChE Journal, 49, 566-577.
[10] Löb, P., Drese, K. S., Hessel, V., Hardt, S., Hofmann, C., Löwe, H., Schenk, R., Schönfeld, F., & Werner, B. (2005). Steering of liquid mixing speed in interdigital micro mixers - From very fast to deliberately slow mixing, Chemical Engineering and Technology, 27, 340-345.
[11] Ducrée, J., Brenner, T., Haeberle, S., Glatzel, T., & Zengerle, R. (2006). Multilamination of flows in planar networks of rotating microchannels, Microfluidics and Nanofluidics, 2, 78-84.
[12] Drese, K., S. (2004). Optimization of interdigital micromixers via analytical modeling - exemplified with the SuperFocus mixer, Chemical Engineering Journal, 101, 403-407.
[13] Wu, Z. and Nguyen, N. T. (2005). Convective-diffusive transport in parallel lamination micromixers, Microfluidics and Nanofluidics, 1, 208-217.
[14] Cerbelli, S. and Giona, M. (2008). On the estimate of mixing length in interdigital micromixers, Chemical Engineering Journal, 138, 523-37.

Table 1: Design parameters and levels used in optimization

Levels	Parameters	
	A(R)	B(D1)
1	10 μm	80 μm
2	20 μm	100 μm
3	30 μm	120 μm

Table 2: Design cases

Cases	Parameters			
	A	B	Mixing efficiency	Pressure drop (kPa)
1	1	1	0.369	7669.17
2	1	2	0.469	8734.20
3	1	3	0.397	7743.10
4	2	1	0.169	7416.98
5	2	2	0.238	7437.03
6	2	3	0.213	7616.58
7	3	1	0.122	7624.73
8	3	2	0.123	7627.36
9	3	3	0.129	7629.85

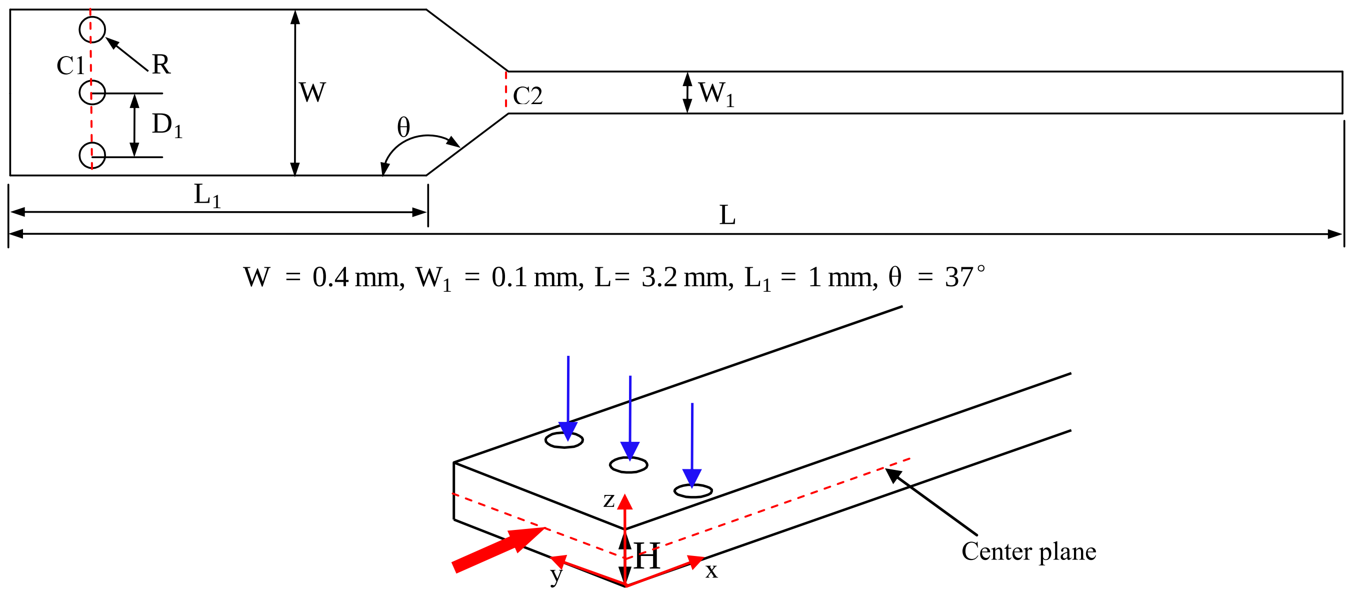

$W = 0.4$ mm, $W_1 = 0.1$ mm, $L = 3.2$ mm, $L_1 = 1$ mm, $\theta = 37^\circ$

H = 0.1 mm

Figure 1: Schematic of perpendicular inlet with focusing section.

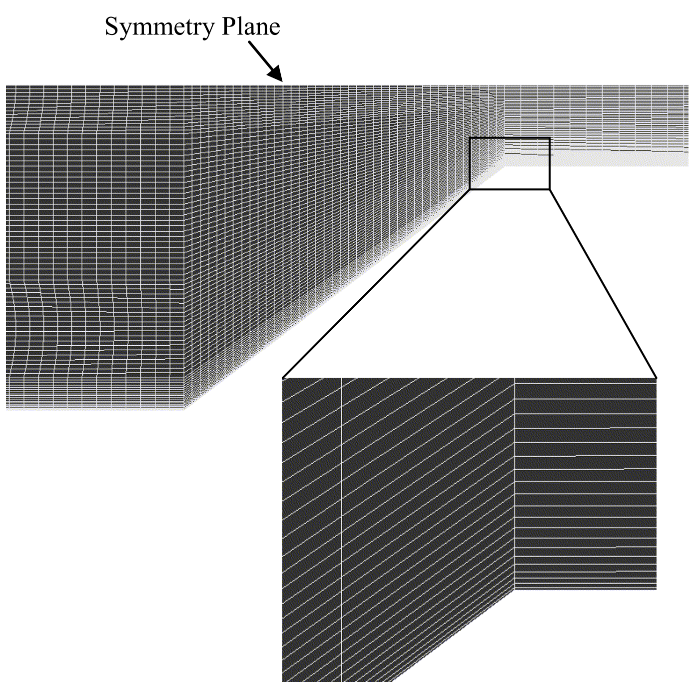

Figure 2: Grid system of half model.

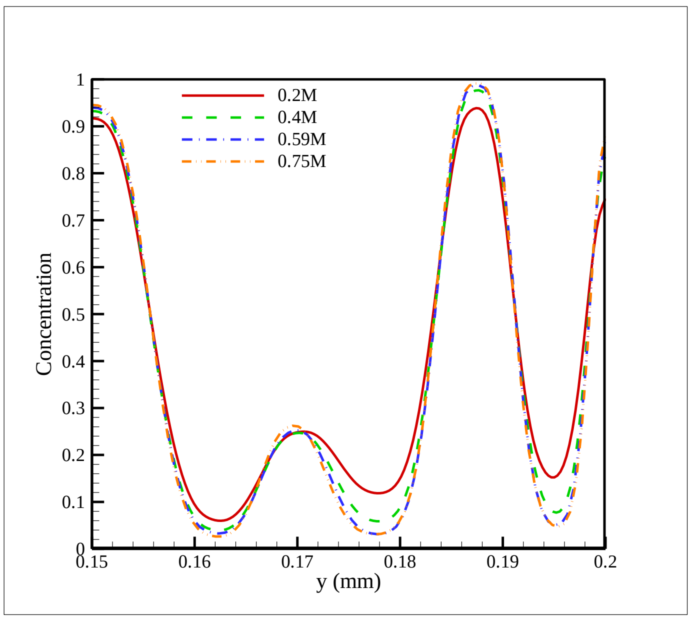

Figure 3: Concentration distribution at the intersection between outlet plane and center plane.

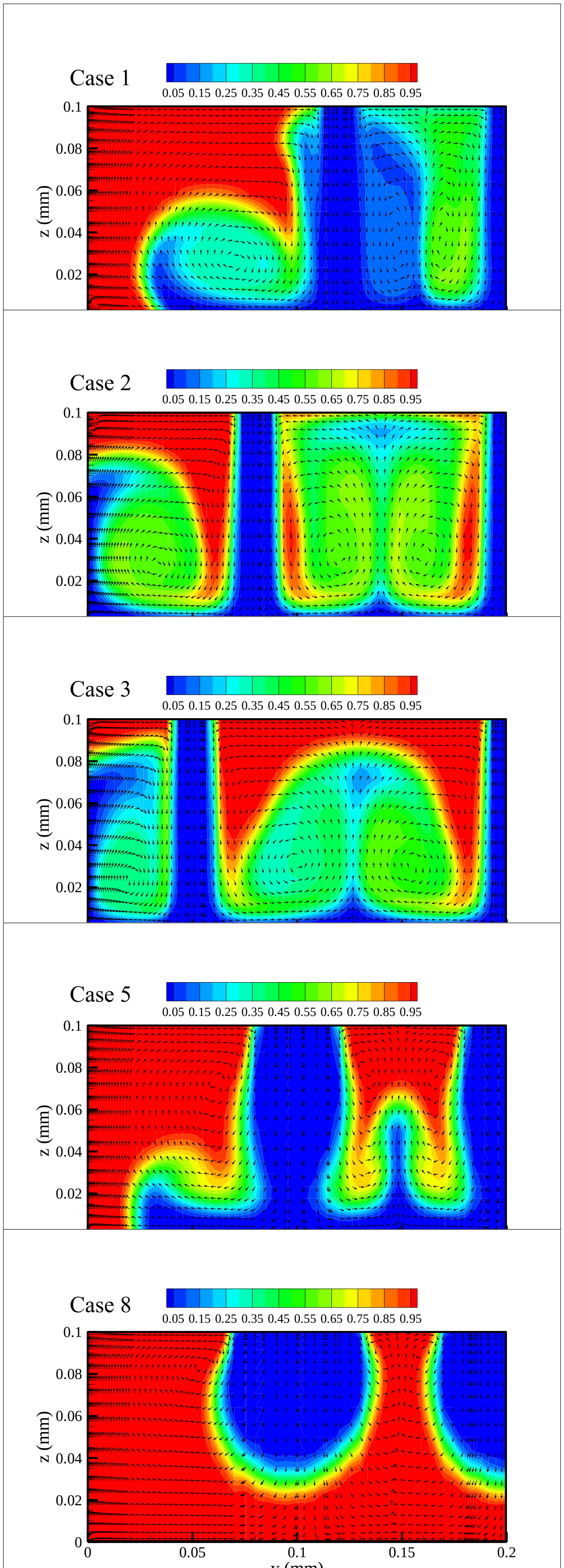

Figure 4: Concentration distributions at C1 for Re = 100.

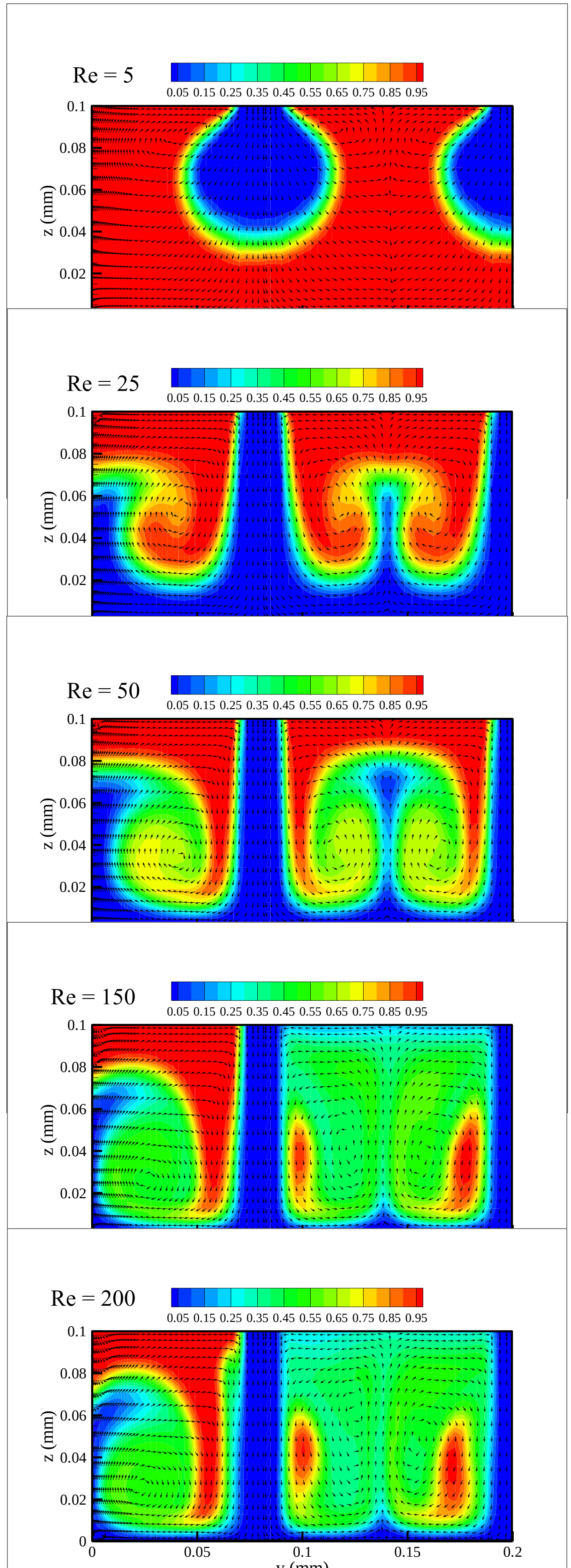

Figure 5: Concentration distributions at C1 at the range of Reynolds number from 5 to 200 in Case 2.

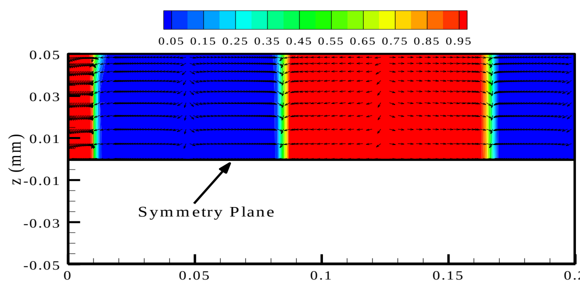

Re = 5

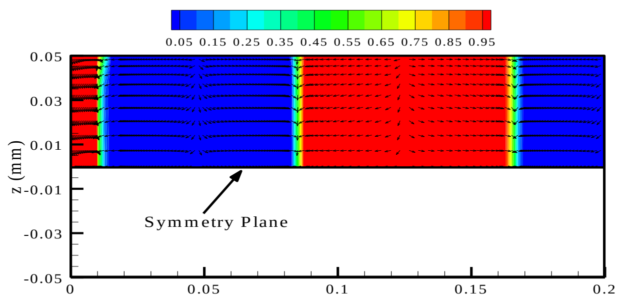

Re = 25

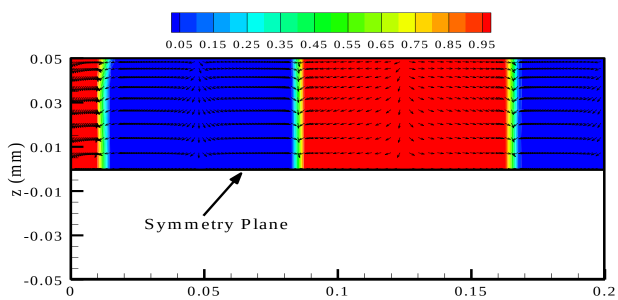

Re = 50

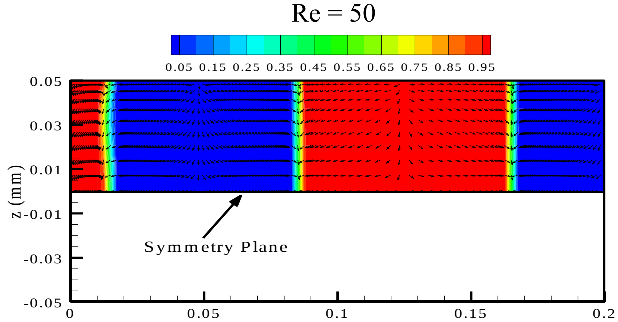

Re = 100

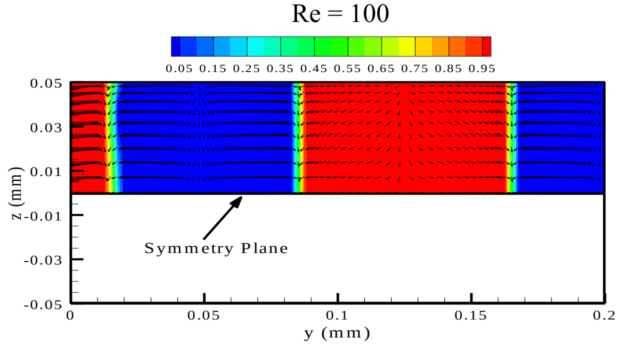

Re = 150

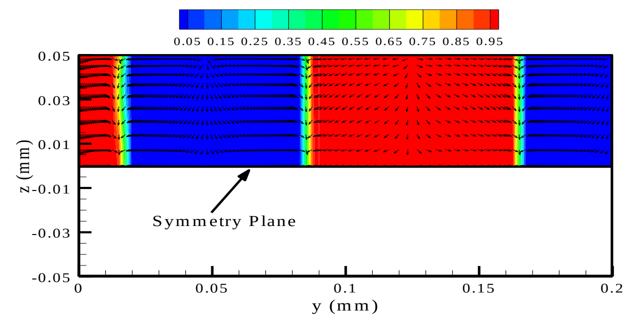

Re = 200

Figure 6: Concentration distributions of parallel lamination inlet at C1.

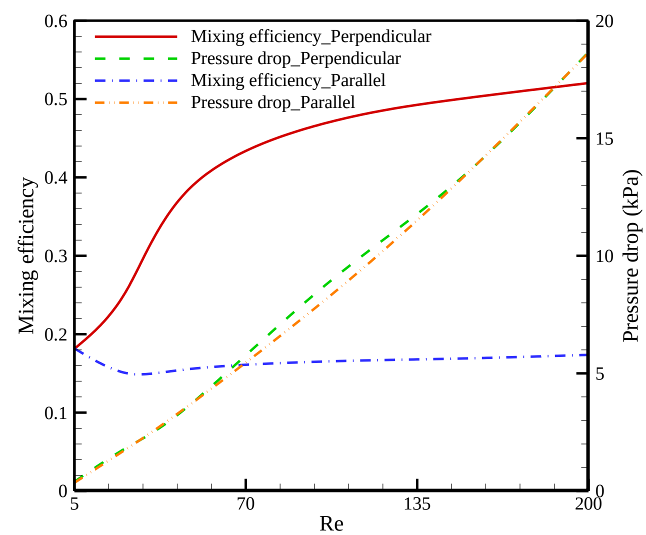

Figure 7: Mixing efficiency and pressure drop at $5 \leq Re \leq 200$.